**Supporting Information**

# Constructing Ru-O-Nb Interfaces in $RuO_x/NbOPO_4$ Nanosheets for One-Pot Conversion of lignin-derived Phenol and Benzyl Alcohol to Polycycloalkane Aviation Biofuels

Danni Liu[a], Kaige Zhang[a], Wenli Zhao[a], Xiaopo Niu[a], Xiangwen Zhang[a], Qingfa Wang[a,b] *

[a]*Key Laboratory for Green Chemical Technology of the Ministry of Education, School of Chemical Engineering and Technology, Tianjin University, Tianjin 300072, P. R. China*
[b]*Zhejiang Institute of Tianjin University, Tianjin University, Ningbo, Zhejiang, 315201, P. R.China*

*Corresponding author.
*E-mail address:* qfwang@tju.edu.cn (Q. Wang); Tel: +86-22-27892340

**Table S1.** Element content of 1-4%$RuO_x$/$NbOPO_4$ catalysts determined by ICP, XPS analysis.

| Element content (Atomic%) | | 1%$RuO_x$/ $NbOPO_4$ | 2%$RuO_x$/ $NbOPO_4$ | 3%$RuO_x$/ $NbOPO_4$ | 4%$RuO_x$/Nb $OPO_4$ | 3%$RuO_x$/S-$NbOPO_4$ |
|---|---|---|---|---|---|---|
| ICP | Ru (wt%) | 1.13 | 2.26 | 3.05 | 3.91 | 3.24 |
| | (Nb/Ru) | 35:1 | 17:1 | 10:1 | 8:1 | - |
| XPS | (Nb/Ru) | 7.9:1 | 7.1:1 | 6.1:1 | 5.3:1 | - |

**Table S2.** Textural properties of the $NbOPO_4$ and $RuO_x$/$NbOPO_4$ catalysts.

| Samples | $NbOPO_4$ | 1%$RuO_x$/ $NbOPO_4$ | 2%$RuO_x$/ $NbOPO_4$ | 3%$RuO_x$/ $NbOPO_4$ | 4%$RuO_x$/ $NbOPO_4$ | 2%$RuO_x$/S-$NbOPO_4$ |
|---|---|---|---|---|---|---|
| [a]Surface area ($m^2\ g^{-1}$) | 41 | 47 | 49 | 51 | 54 | 39 |
| [b]Pore volume ($cm^3.g^{-1}$) | 0.30 | 0.24 | 0.21 | 0.20 | 0.13 | 0.22 |

[a]BET surface Area.

[b]$P/P_0$=0.99 adsorption cumulative volume of pores.

**Table S3.** The acid type, acid amount, $n_{Ru}$ and $n_{Ru}/n_{BAS}$ of the $RuO_x/NbOPO_4$ samples.

| Catalysts | Acidity (μmol $g^{-1}$) | | | | | $^{c}n_{Ru}$ (μmol $g^{-1}$) |
|---|---|---|---|---|---|---|
| | $^{a}$Brønsted acid sites (μmol $g^{-1}$) | $^{a}$Lewis acid sites (μmol $g^{-1}$) | $^{a}$Total: B +L (μmol $g^{-1}$) | $^{a}$B/L (ratio) | $^{b}$Acidic sites (mmol $g^{-1}$) | |
| 1%$RuO_x/NbOPO_4$ | 58.13 | 23.50 | 81.64 | 2.47 | 0.63 | 39.50 |
| 2%$RuO_x/NbOPO_4$ | 36.41 | 17.81 | 54.21 | 2.04 | 0.47 | 48.23 |
| 3%$RuO_x/NbOPO_4$ | 23.46 | 17.41 | 40.87 | 1.35 | 0.60 | 59.37 |
| 4%$RuO_x/NbOPO_4$ | 20.22 | 17.51 | 37.73 | 1.15 | 0.76 | 60.89 |
| 3%$RuO_x$/S-$NbOPO_4$ | 8.59 | 39.49 | 48.07 | 0.22 | 0.77 | - |
| modified $NbOPO_4$ | 25.38 | 30.96 | 55.34 | 0.79 | - | - |

[a]Measured by Py-IR.

[b]Measured by $NH_3$-TPD.

[c]The mole of surface ruthenium atoms ($n_{Ru}$) was calculated by $H_2$-TPD.

**Table S4.** The acid type and acid amount of the $Nb_2O_5$ samples.

| Catalysts | Acidity (μmol $g^{-1}$) | | |
|---|---|---|---|
| | $^{a}$Brønsted acid sites (μmol $g^{-1}$) | $^{a}$Lewis acid sites (μmol $g^{-1}$) | $^{a}$Total: B +L (μmol $g^{-1}$) |
| $Nb_2O_5$-300 | 0.18 | 9.25 | 9.43 |
| $Nb_2O_5$-400 | 0.19 | 9.14 | 9.33 |

**Table S5.** The acid type, acid amount the 5%Ru/C and 3%$RuO_x$/$NbOPO_4$ samples.

| **Samples** | [a]Brønsted acid sites (μmol $g^{-1}$) | [a]Lewis acid sites (μmol $g^{-1}$) | [a]Total: B +L (μmol $g^{-1}$) | [a]B/L (ratio) | [b]Acidic sites (mmol $g^{-1}$) |
|---|---|---|---|---|---|
| 5%Ru/C | 7.25 | 29.54 | 36.79 | 0.24 | 1.90 |
| 3%$RuO_x$/$NbOPO_4$ | 23.46 | 17.41 | 40.87 | 1.35 | 0.60 |

[a]Measured by Py-IR.

[b]Measured by $NH_3$-TPD.

**Table S6.** The reaction rates of BP hydrogenation and OCI cyclisation hydrogenation at different temperatures.

| Temperature / °C | 100 | 110 | 120 | 130 |
|---|---|---|---|---|
| $R_1*10^2$ / mol·$L^{-1}$·$min^{-1}$ | 5.68 | 11.23 | 15.04 | 21.83 |
| $R_2*10^2$ / mol·$L^{-1}$·$min^{-1}$ | 3.79 | 7.04 | 9.44 | 19.10 |

**Table S7.** The reaction rates of BP hydrogenation and OCI cyclisation hydrogenation at different pressures.

| $H_2$ Pressure / MPa | 3 | 4 | 5 | 6 |
|---|---|---|---|---|
| $R_1*10^2$ / mol·$L^{-1}$·$min^{-1}$ | 4.46 | 8.05 | 9.94 | 12.9 |
| $R_2*10^2$ / mol·$L^{-1}$·$min^{-1}$ | 2.47 | 5.34 | 6.65 | 7.51 |

**Table S8.** The reaction rates of BP hydrogenation and OCI cyclisation hydrogenation at different BP concentrations.

| BP Concentration / mol $L^{-1}$ | 0.10 | 0.13 | 0.17 | 0.20 |
|---|---|---|---|---|
| $R_1*10^2$ / mol·$L^{-1}$·$min^{-1}$ | 5.94 | 7.61 | 11.23 | 6.73 |
| $R_2*10^2$ / mol·$L^{-1}$·$min^{-1}$ | 3.49 | 4.92 | 7.04 | 4.79 |

**Table S9.** The rate constants of the BP and OCI hydrogenation reaction at different temperatures.

| Temperature / ℃ | 100 | 110 | 120 | 130 |
|---|---|---|---|---|
| $k_1*10^2$ | 6.43 | 12.71 | 17.03 | 24.72 |
| $k_2*10^2$ | 11.90 | 22.11 | 29.65 | 60.00 |

$$R_1 = k_1[BP]^{1.23}[H_2]^{1.50}$$
$$R_2 = k_2[OCI]^{1.32}[H_2]^{1.60}$$

**Table S10.** Kinetic parameters of different steps in BP HDO over 3%$RuO_x$/$NbOPO_4$ catalyst.

| reaction steps | Ea (kJ $mol^{-1}$) | A |
|---|---|---|
| BP hydrogenation | 54.29 | exp (14.86) |
| OCI cyclization hydrogenation | 64.26 | exp (18.59) |

**Table S11.** The green chemistry metrics for the alkylation reaction and HDO reaction individually.

| Reaction | [a] E-factor | [b]Ideal atom economy | [c]Effective atom economy | [d] Carbon efficiency |
|---|---|---|---|---|
| Alkylation | 2.28 | 91.2% | 30.4% | 33.59% |
| HDO | 0.31 | 89.9% | 79.1% | 88% |

[a] *E*-factor = [$m_{reactants}$ + $m_{solvent}$+ $m_{H2O}$- $m_{products}$] / $m_{products}$

[b] Ideal atom economy = [molar mass of the target product / sum of the molar masses of all reactants] × 100%

[c] Effective atom economy = [mass of the target product actually obtained / total mass of all reactants fed] × 100%

[d] Carbon efficiency = [mass of the target product actually obtained / total mass of all reactants fed] × 100%

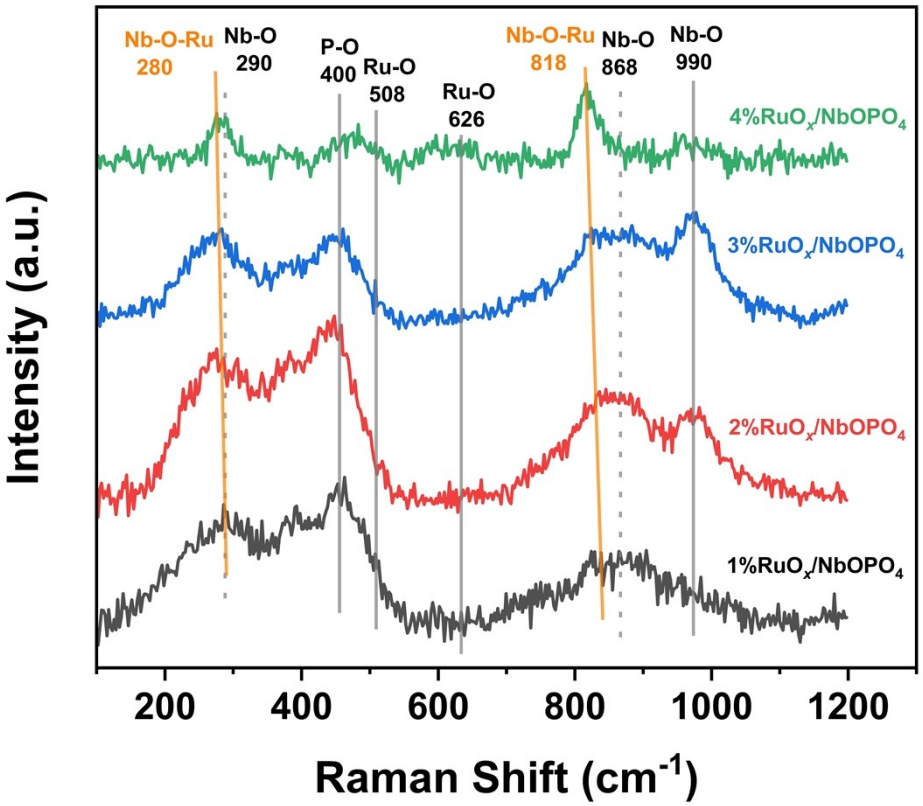


**Fig. S1.** Typical Raman images of 1-4%$RuO_x$/$NbOPO_4$.

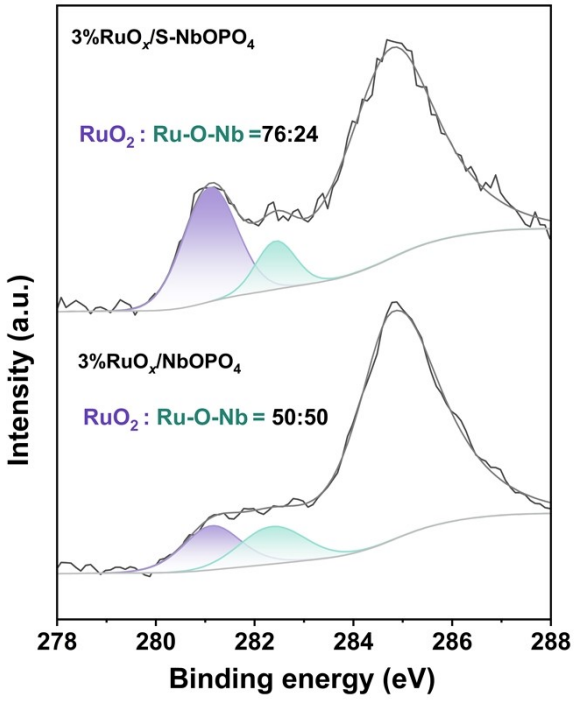


**Fig. S2.** Ru 3d XPS spectra of 3%$RuO_x$/$NbOPO_4$ and 3%$RuO_x$/S-$NbOPO_4$.

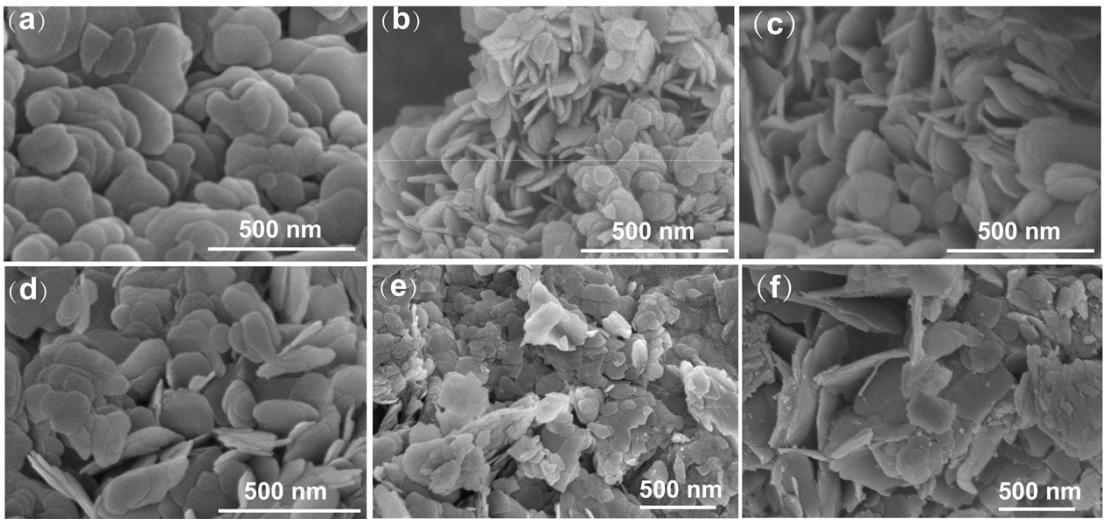


**Fig. S3.** Typical SEM images of (a) $NbOPO_4$-W, (b) S-$NbOPO_4$, (c) 1%$RuO_x$/$NbOPO_4$, (d) 2%$RuO_x$/$NbOPO_4$, (e) 3%$RuO_x$/$NbOPO_4$, (f) 4%$RuO_x$/$NbOPO_4$.

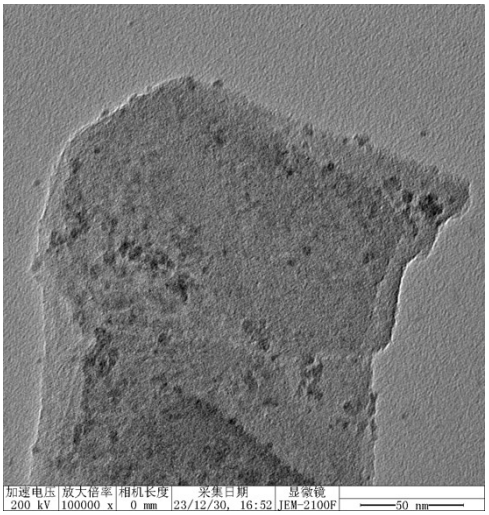


**Fig. S4.** TEM images of 3%$RuO_x$/S-$NbOPO_4$.

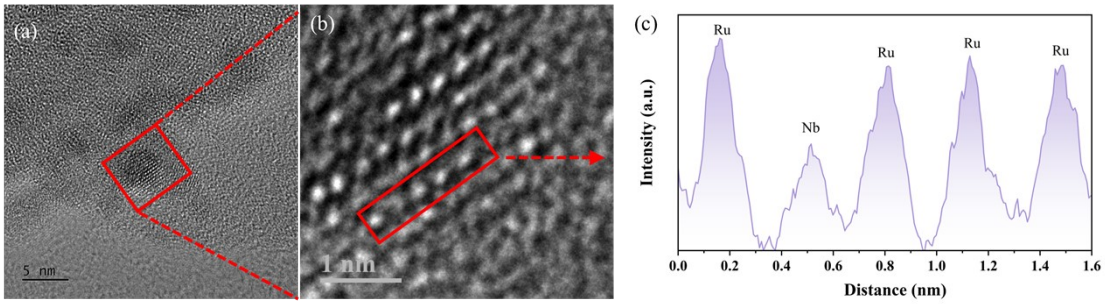


**Fig. S5.** (a, b) TEM images of 3%$RuO_x$/$NbOPO_4$. (c) Line scan measured along the rectangular regions.

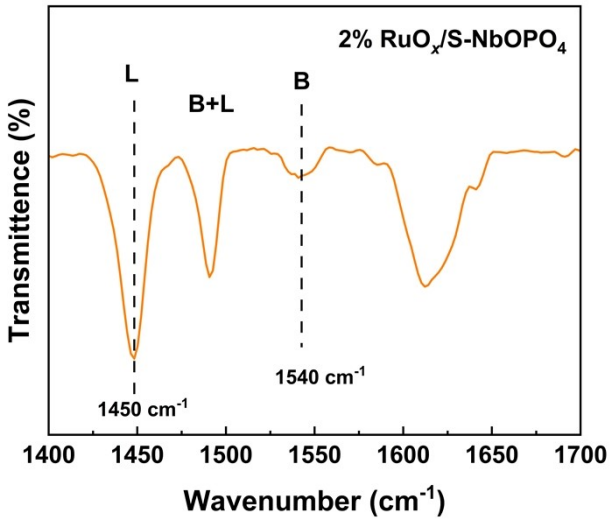


**Fig. S6.** Py-IR spectra of 3%$RuO_x$/S-$NbOPO_4$.

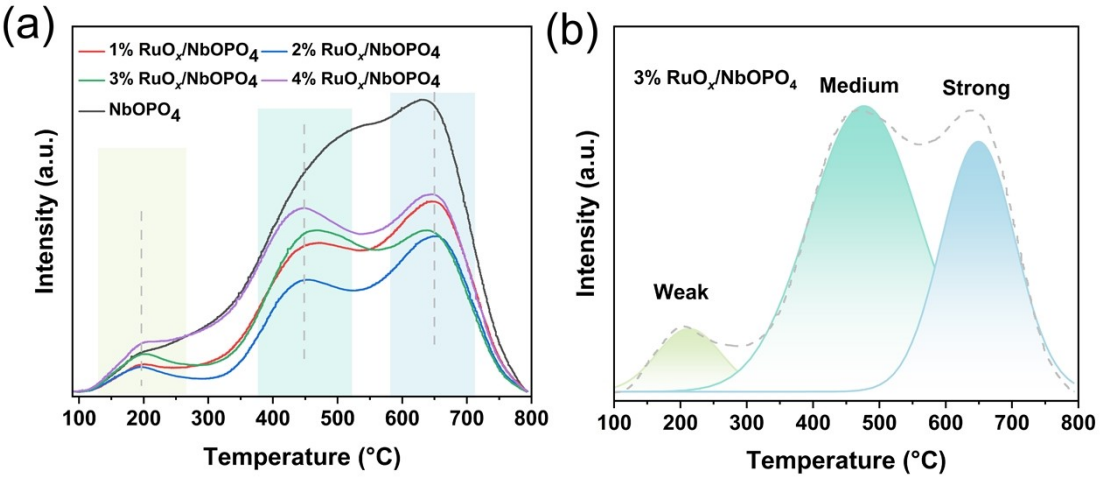


**Fig. S7.** (a) $NH_3$-TPD of $NbOPO_4$ and1-4%$RuO_x$/$NbOPO_4$, (b) $NH_3$-TPD of 3%$RuO_x$/$NbOPO_4$.

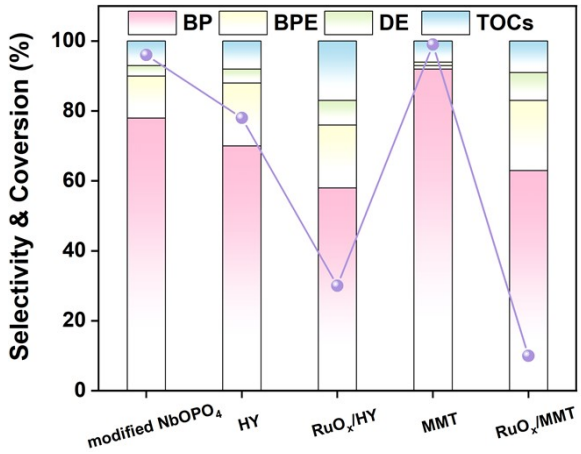


**Fig. S8.** Catalytic performance in BA conversion and alkylation product selectivity.

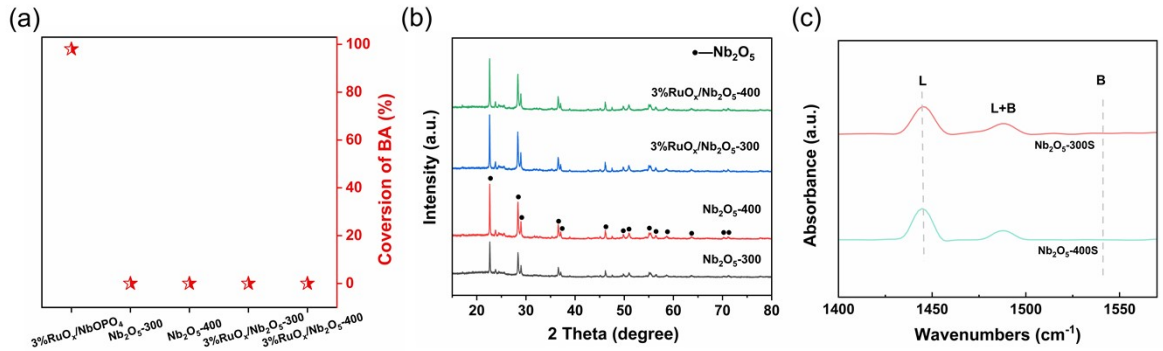


**Fig. S9.** (a) Catalytic performance in BA conversion with different catalysts. Reaction conditions: 5.8 mmol BA, 23.3 mmol phenol, 3.5 wt% catalyst. Alkylation: 130 °C for 2 h. (b) XRD spectra of $Nb_2O_5$-300, $Nb_2O_5$-400, 3%$RuO_x$/$Nb_2O_5$-300 and 3%$RuO_x$/$Nb_2O_5$-400. (c) Py-IR of $Nb_2O_5$-300 and $Nb_2O_5$-400.

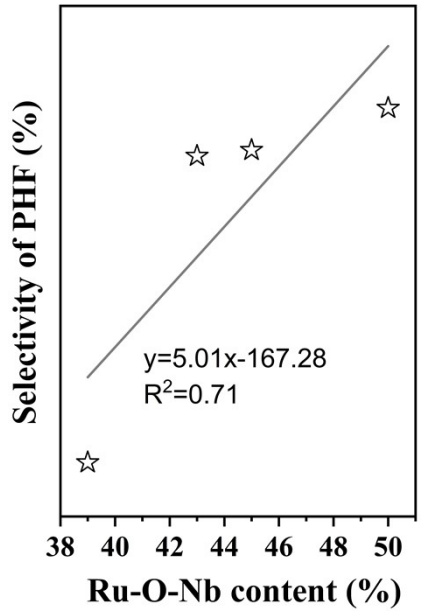


**Fig. S10.** Selectivity of PHF as a function of Ru-O-Nb content.

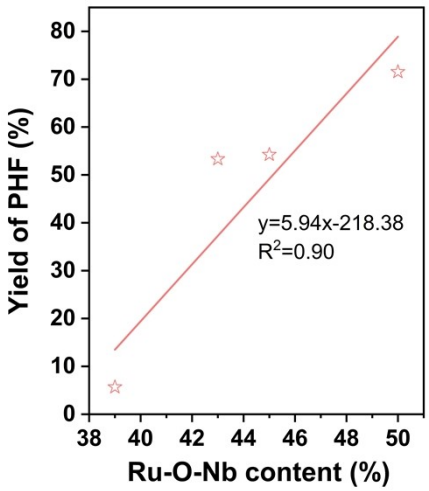


**Fig. S11.** Yield of PHF as a function of Ru-O-Nb content.

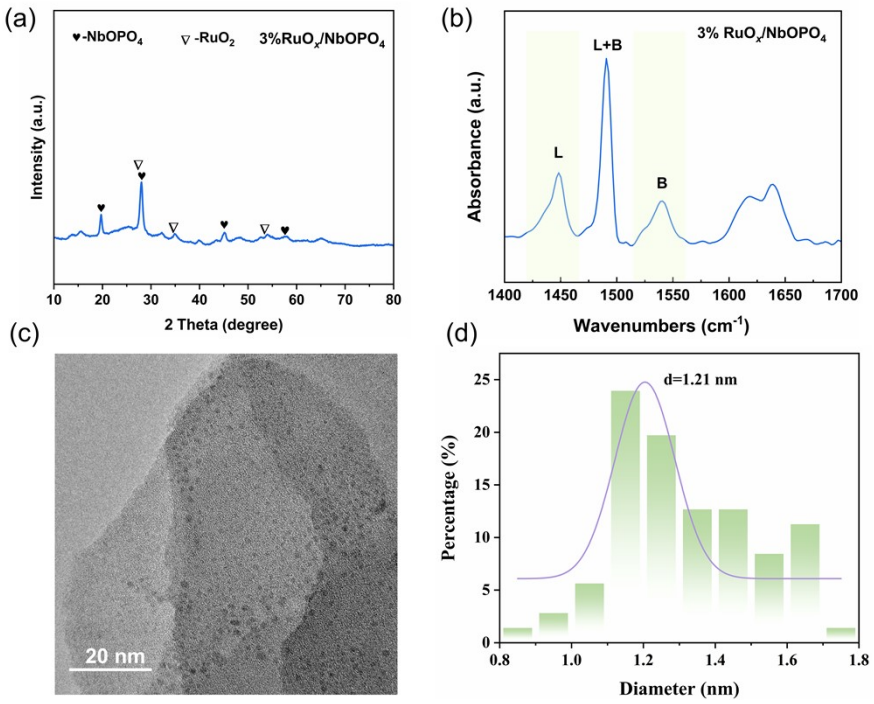


**Fig. S12.** (a) XRD (b) Py-IR (c) TEM and (d) Ru nanoparticle size distributions of reused 3%$RuO_x$/$NbOPO_4$ catalysts.

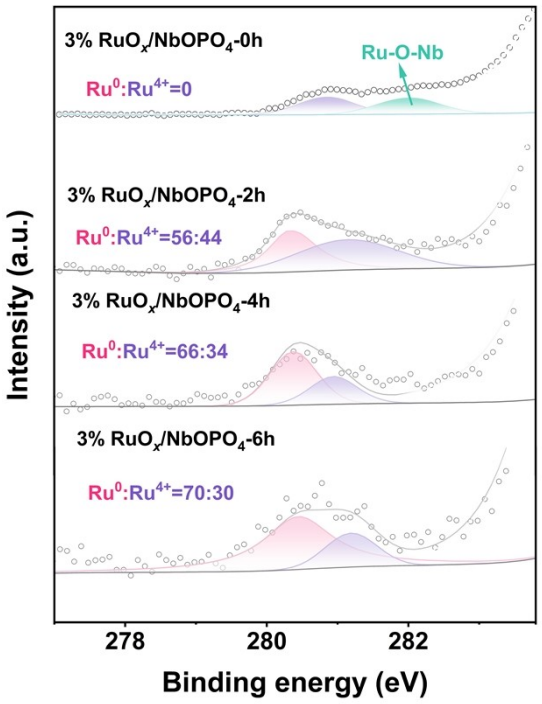


**Fig. S13.** XPS spectra of Ru 3d during HDO reactions.

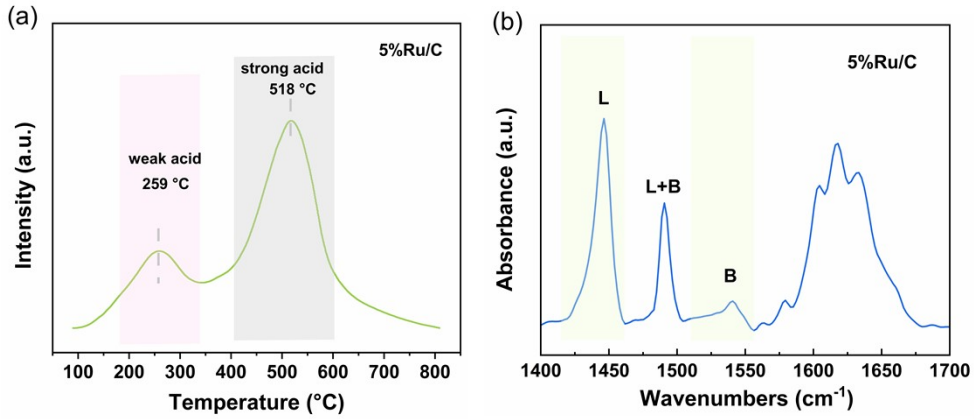


**Fig. S14.** (a) Py-IR and $NH_3$-TPD of 5%Ru/C.

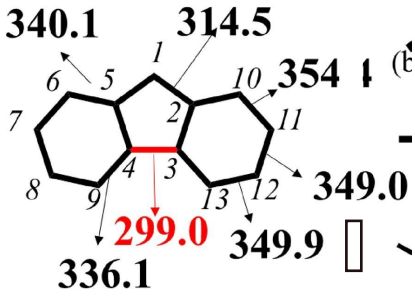


**Fig. S15.** Dissociation enthalpies (kJ/mol) from PHF to relevant free radicals.

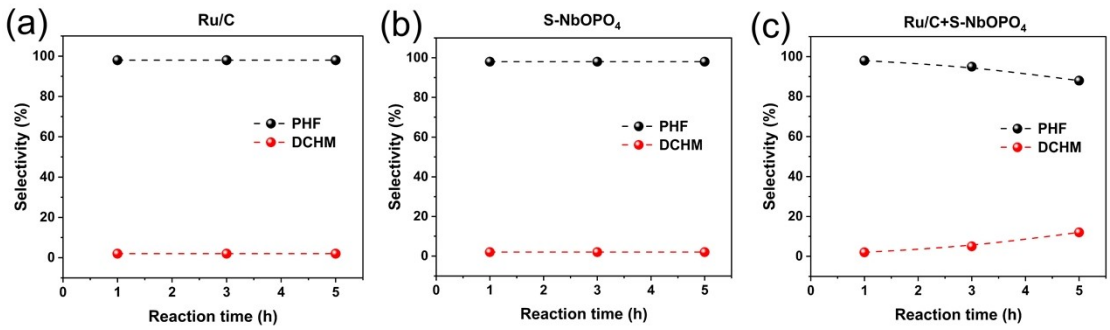


**Fig. S16.** Selectivity of PHF and DCHM with 2BP over (a) 5% Ru/C, (b) S-$NbOPO_4$, (c) 5% Ru/C + S-$NbOPO_4$.

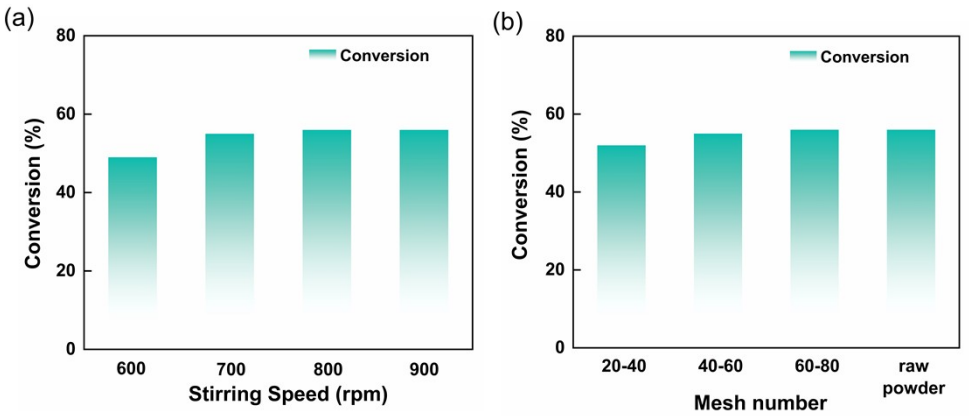


**Fig. S17.** (a) Conversion of BP at different stirring speeds. Reaction conditions: 0.025 g of catalysts, 2.5 mmol of BP, 4 MPa $H_2$, 120 °C. (b) Conversion of BP at different catalyst size. Reaction conditions: 0.025 g of catalysts, 800 rpm, 2.5 mmol of BP, 4 MPa $H_2$, 120 °C.

The effect of different stirring speeds on the reaction process is shown in Fig. S14a. The experimental results indicate that when the stirring speed is increased above 700 rpm, the conversion of BP remains essentially constant. To ensure the neglect of external diffusion influences, a stirring speed of 800 rpm was selected for subsequent experiments. Four sizes of catalyst powders, i.e., 20-40 mesh (average particle size dP = 0.64 mm), 40-60 mesh (dP = 0.34 mm), 60-80 mesh (dP = 0.22 mm), and raw powder are used to check the effect of the internal diffusion resistance. It is found from Fig. S17 that the internal diffusion limitation can be ignored when the catalyst size is reduced to 0.34 mm. Moreover, since the raw powder catalyst particle size was >80 mesh (approximately 98%), internal diffusion effects were considered negligible under the given stirring conditions.

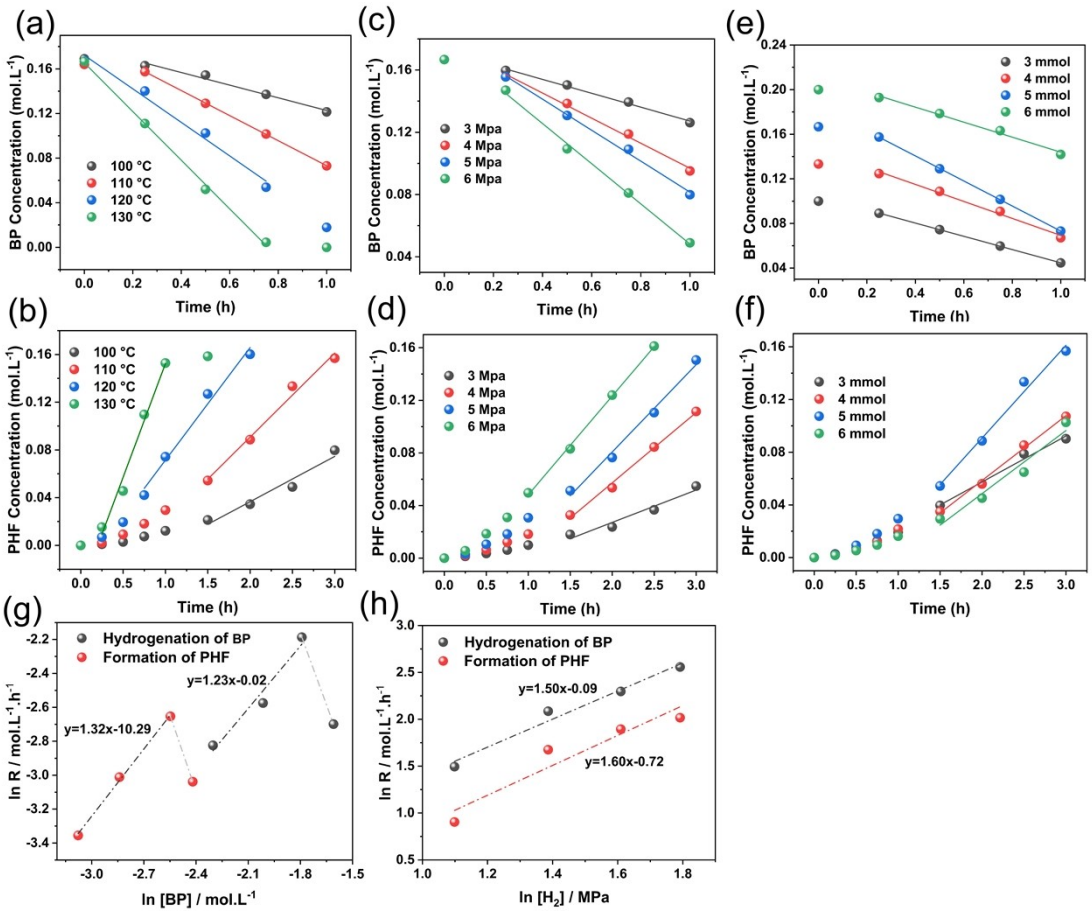


**Fig. S18.** Reaction concentrations of BP and PHF as a function of time, (a) BP hydrogenation reaction rate at different temperatures, (b) OCI cyclisation hydrogenation reaction rate at different temperatures, (c) BP hydrogenation reaction rate at different pressures, (d) OCI cyclisation hydrogenation reaction rate at different pressures, (e) BP hydrogenation reaction rate at different BP initial concentrations, (f) OCI cyclisation hydrogenation reaction rate at different BP initial concentrations, (g) Reaction rate as a function of BP and OCI concentration, (h) Reaction rate as a function of $H_2$ pressure.

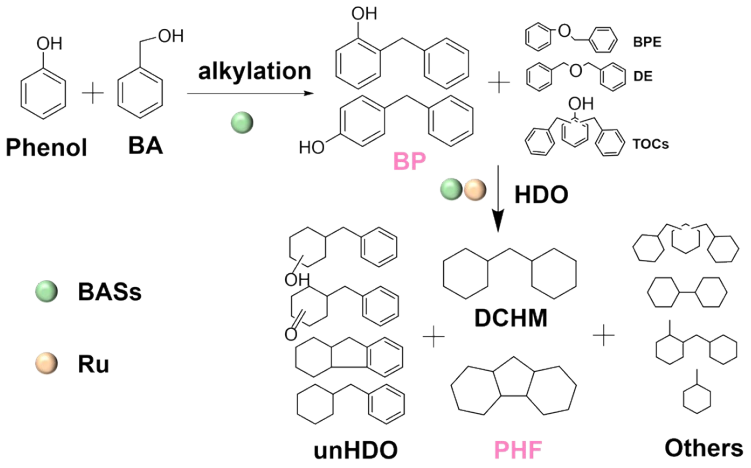


**Fig. S19.** Proposed reaction pathways for alkylation and HDO processes.

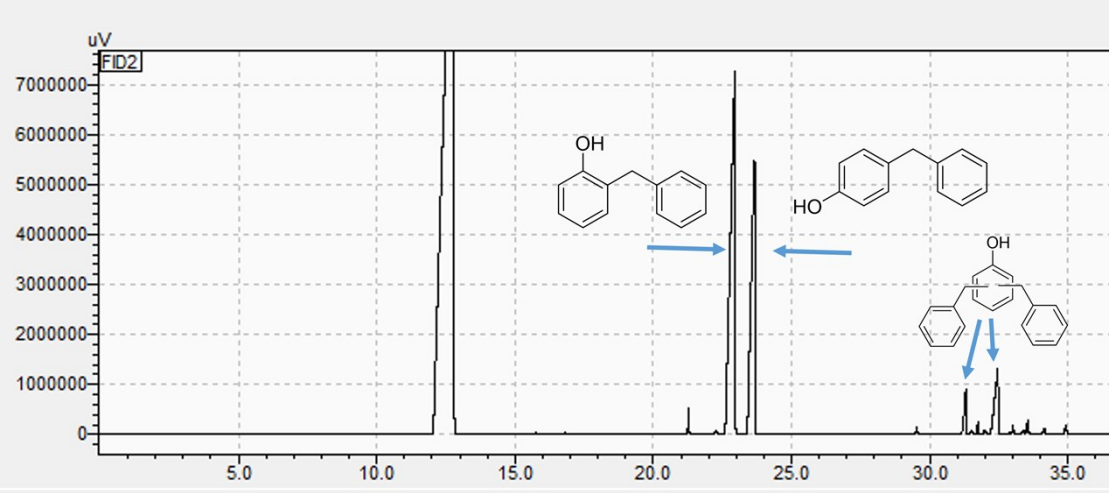


**Fig. S20.** Gas chromatogram of the alkylation products of ont-pot over 3%$RuO_x$/$NbOPO_4$ catalyst. Reaction conditions: 139.8 mmol phenol, 34.8 mmol BA,3.5 wt% 3%$RuO_x$/$NbOPO_4$ catalyst, 130 °C, 2 h.

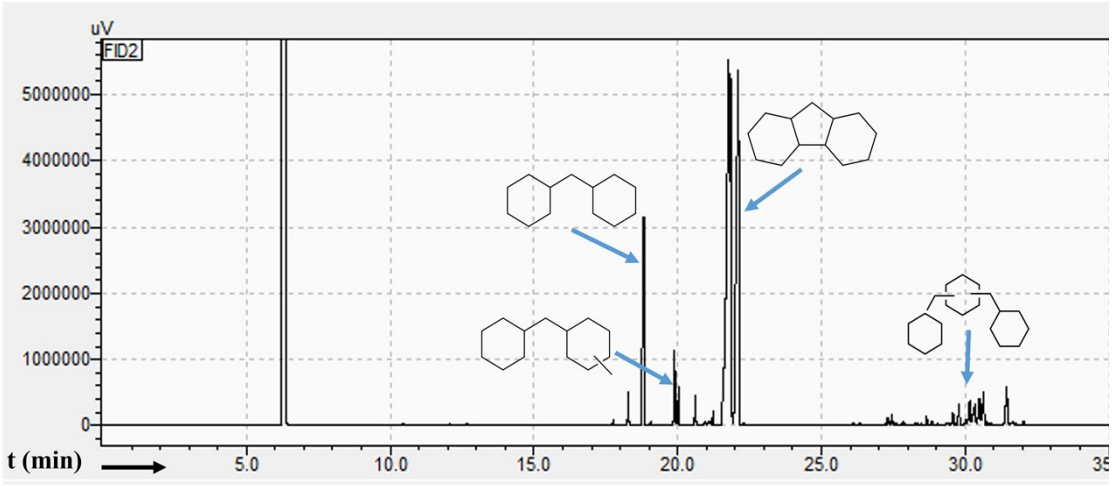


**Fig. S21.** Gas chromatogram of the HDO products of ont-pot over 3%$RuO_x$/$NbOPO_4$ catalyst after simple vacuum distillation.
Reaction conditions: unpurified alkylation products, 3.5 wt% 3%$RuO_x$/$NbOPO_4$, 160 °C, 1 h.

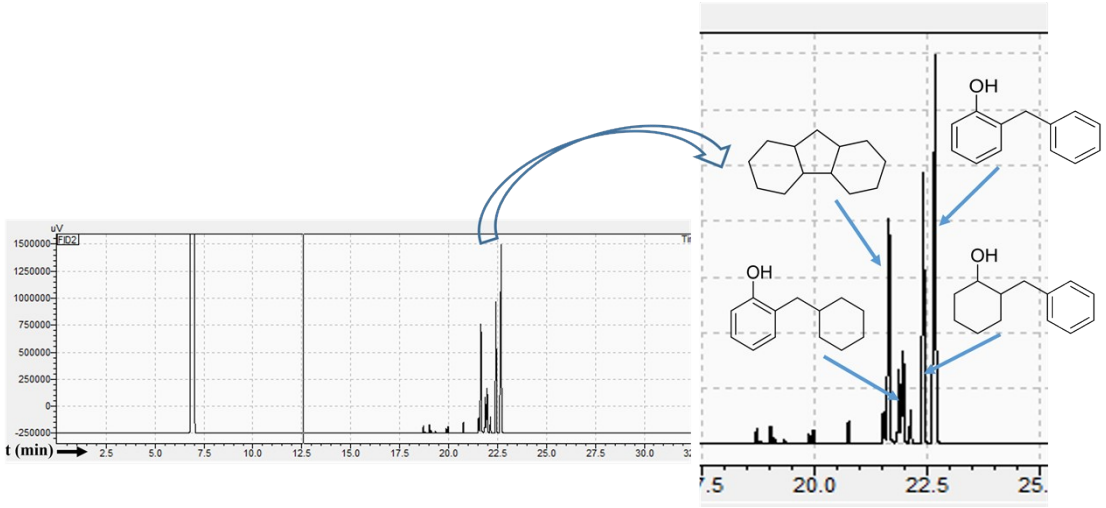


**Fig. S22.** Gas chromatogram of the HDO products of 2BP over 3%$RuO_x$/$NbOPO_4$ catalyst.

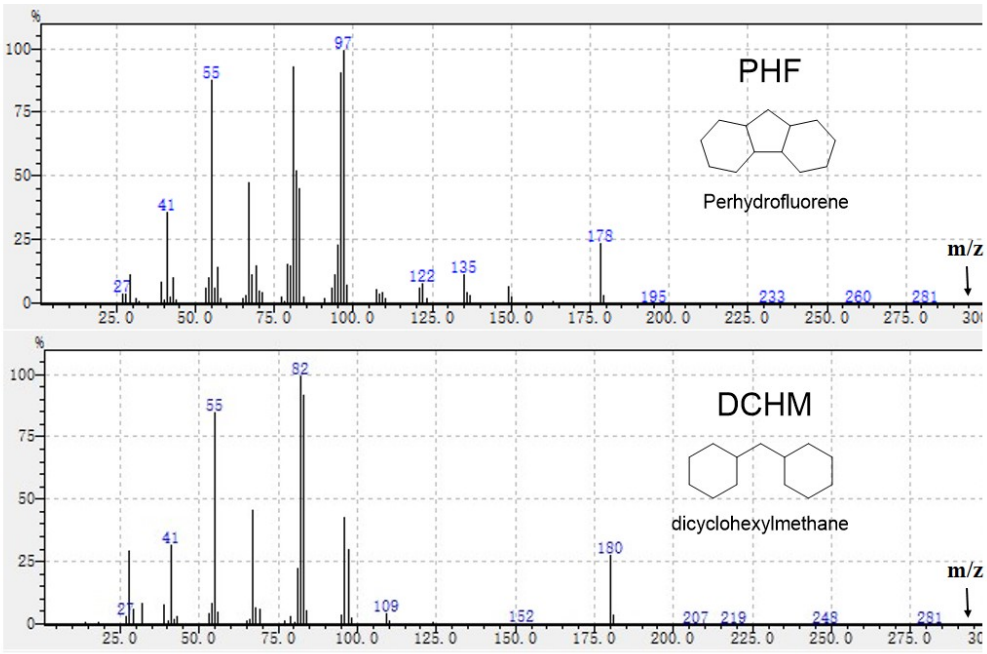


**Fig. S23.** Mass spectrograms of PHF and DCHM.

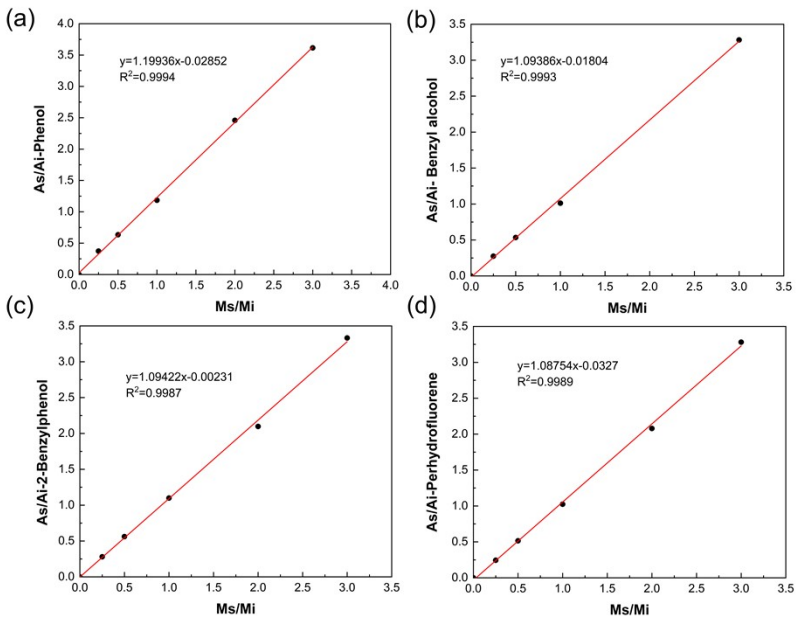


**Fig. S24.** The calibration curve of standard material to (a) Phenol, (b) Benzyl alcohol, (c) 2-Benzylphenol, (d) Perhydrofluorene.

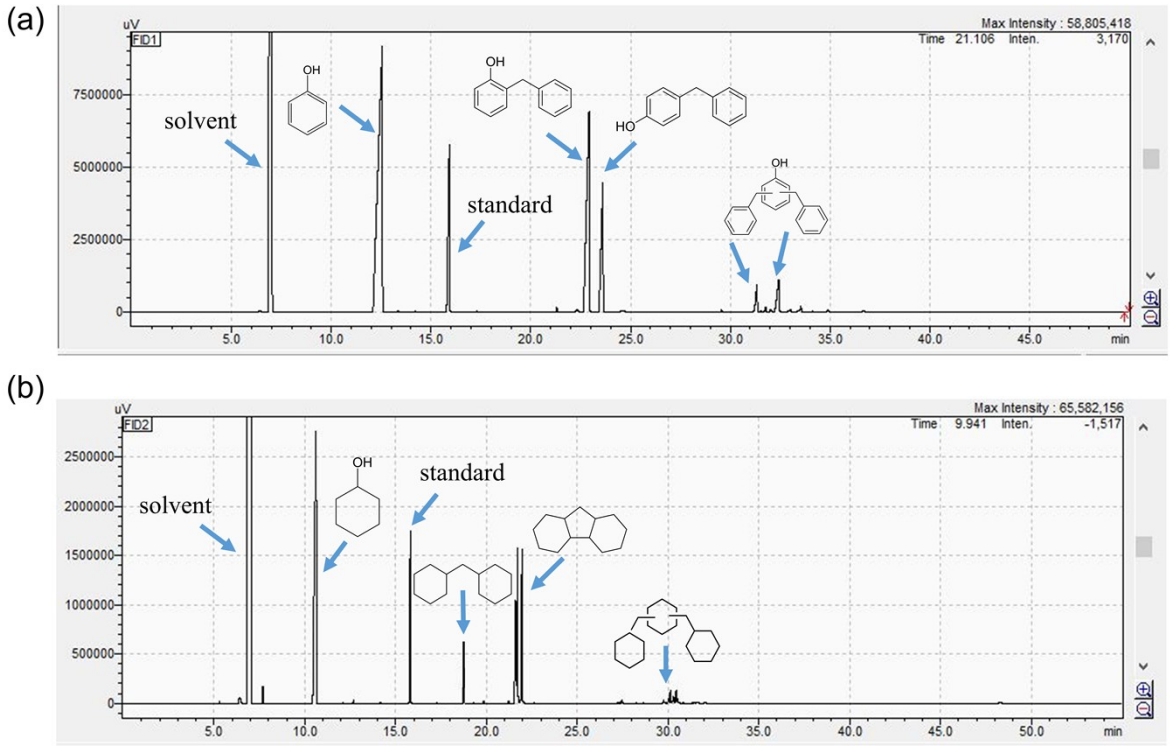


**Fig. S25.** Gas chromatogram of (a) the alkylation products of one-pot over 3%$RuO_x$/$NbOPO_4$ catalyst. Reaction conditions: 139.8 mmol phenol, 34.8 mmol BA, 3.5 wt% 3%$RuO_x$/$NbOPO_4$ catalyst, 160 °C, 2 h. (b) The HDO products. Reaction conditions: The unpurified alkylation products, 160 °C, 1 h, 6 MPa.